Pis'ma v ZhETF, vol.60, iss.9, pp.659 - 665

THE INTERSECTION OF A VORTEX LINE WITH A TRANSVERSE SOLITON PLANE IN ROTATING ^{3}He-A: π_3 TOPOLOGY

V.M.H.Ruutu[+], *Ü.Parts*[+], *J.H.Koivuniemi*[+], *M.Krusius*[+], *E.V.Thuneberg*[+], *G.E.Volovik*[+*]

[+]*Low Temperature Laboratory, Helsinki University of Technology*
02150 Espoo, Finland

[*]*Landau Institute for Theoretical Physics*
117334 Moscow, Russia

Submitted 17 October, 1994

The coexistence of two continuous textures of different dimensionality is observed in the A-phase of superfluid ^{3}He: nonsingular 4π vortex lines crossing a planar transverse soliton. The nontrivial π_3 topology of the intersection point is discussed in terms of the linking numbers.

Several types of coexistence of topological defects of different dimensionality have been found in condensed matter with broken symmetry. (i) An object of lower dimensionality may serve as a boundary for a higher dimensional object. Examples of this type are a monopole as a termination point of a disclination line in liquid crystals [1], a cosmic domain wall with a string as its edge line [2], an antiphase boundary terminating on a dislocation line in ordered binary alloys [3], a planar soliton in superfluid ^{3}He-B emanating from a vortex line [4], etc. (ii) An object of lower dimensionality may exist within a higher dimensional object, from where it cannot escape to the world outside. Examples of this type are a Bloch line within a domain wall in ferromagnets [3], and the vortex sheet in ^{3}He-A, which is a 2-dimensional soliton with accumulated 1-dimensional continuous vortices [5, 6].

Here we report on an observation of another type of topological interaction: (iii) a nonsingular vortex line crossing a transverse planar soliton (Fig.1). As distinct from the geometry of the vortex sheet, in which the vortices are parallel to the soliton wall, in the present geometry the vortex and the soliton have only zero-dimensional common region - the intersection point. The intersection represents a point-like object, which is singularity-free, since singularities are not created easily in a rotating container. Point-like continuous objects, which are usually described by the π_3 homotopy group, were discussed in many areas of physics: particle-like solitons in the phases A and B of superfluid ^{3}He [7–9]; "textures" or Skyrmions in particle physics and cosmology [2, 10]; "configurations" [11, 12] or "semi-defects"[13] in liquid crystals; solitons in ordered magnets[14], etc. In all cases such an object should collapse due to energetic reason to zero size. (In some cases the stabilization at some length scale is however suggested: this length can be produced (i) by the higher gradient terms in energy [8], (ii) by dynamical conservation of the some physical quantity which fixes the size of the soliton [7, 14], or (iii) by some natural scale like the cholesteric pitch [15]). In our case the twisting of the $\hat{\mathrm{I}}$ texture within the soliton, ie. the nontrivial π_1 topology of the soliton, together with the nontrivial π_2 topology of the $\hat{\mathrm{I}}$ texture within

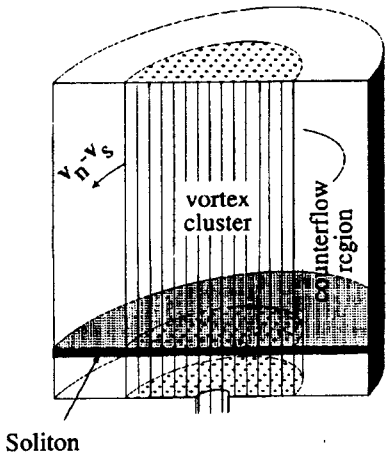

Рис.1

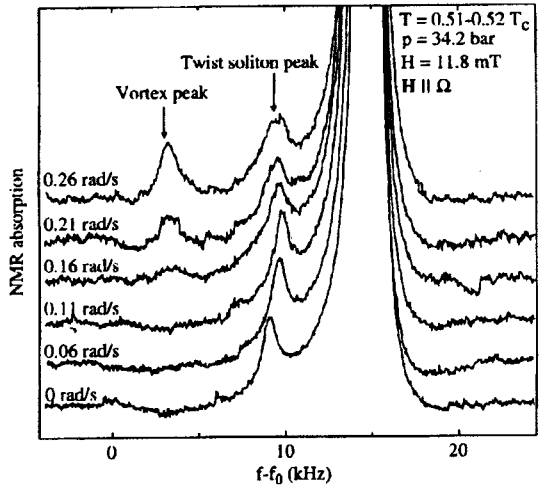

Рис.2

Fig.1. A cluster of vortices crossing a transverse soliton. The cluster is surrounded by a vortex-free region with nonzero counterflow $\vec{v}_s - \vec{v}_n$. The counterflow influences the position of the soliton peak in accordance with Fig.3

Fig.2. cw NMR absorption as a function of the frequency shift $\Delta f = f - f_0$ from the Larmor frequency f_0 for 6 different rotation velocities Ω. The data are recorded in one continuous run in which the rotation velocity is increased from zero to the maximal velocity $\Omega_m = 0.26$ rad/s, while the transverse twist soliton is in the container.

the vortex, necessarily produce the nontrivial π_3 topology of $\hat{\mathbf{l}}$ in the intersection of these planar and linear objects.

A soliton in ^{3}He-A is a wall between domains with parallel $\hat{\mathbf{l}} = \hat{\mathbf{d}}$ and antiparallel $\hat{\mathbf{l}} = -\hat{\mathbf{d}}$ orientations of the A-phase orbital $\hat{\mathbf{l}}$ and magnetic $\hat{\mathbf{d}}$ anisotropy axes. A soliton, whose plane is oriented normal to the magnetic field direction $\mathbf{H} \parallel \hat{z}$, is the so called composite twist soliton, in which the axes $\hat{\mathbf{l}}$ and $\hat{\mathbf{d}}$ are twisted in opposite directions[16]: $\hat{\mathbf{l}}_{\rm soliton}(z) = \hat{x}\cos\alpha(z) + \hat{y}\sin\alpha(z)$, $\hat{\mathbf{d}}_{\rm soliton}(z) = \hat{x}\cos\beta(z) + \hat{y}\sin\beta(z)$, with $\alpha(+\infty) - \beta(+\infty) = \alpha(-\infty) - \beta(-\infty) + \pi$.

The soliton often appears after cool-down into the superfluid state. Its existence is displayed in cw NMR experiments as a satellite peak in the NMR absorption as a function of excitation frequency f (see Fig.2). The frequency of an absorption maximum is conventionally expressed as $f^2 = f_0^2 + R^2 f_\parallel^2$, where $f_0 = \gamma H/2\pi$ is the Larmor frequency and $f_\parallel$ the temperature and pressure dependent longitudinal resonance frequency of the A phase. The dominant peak at $R = 1$ originates from the dipole-locked ($\hat{\mathbf{l}} = \pm\hat{\mathbf{d}}$) bulk liquid. The low-frequency satellite peak in the stationary container at $\Omega = 0$ arises from a spin-wave mode that is localized in the core of the soliton, where the dipole-unlocked texture, $\hat{\mathbf{d}} \neq \pm\hat{\mathbf{l}}$, produces an attractive potential. The orientation of the soliton can be extracted from the position of the peak[5]: the value $R^2_{\rm sol} = 0.613$ at $\Omega = 0$ is the signature of the horizontal composite twist soliton. All measurements are for the magnetic field H parallel to the axis $\hat{z}$ of the cylindrical container at a temperature $T = 0.5\,T_c$ and pressure $p = 34.2$ bar. The experimental technique is the same as in Ref. [5].

In previous experiments at $T \sim 0.7 - 0.8\ T_c$ the twist soliton was swept out by rotation, as distinct from the vertical soliton, which gives rise to the vortex sheet [5]. At lower temperature $T \sim 0.5\ T_c$, the transverse soliton does not disappear under rotation and remains in the container even when vortices appear. The change in the soliton structure under rotation is reflected in the dependence of R^2_{sol} on the angular velocity Ω of rotation in Fig.3. First the frequency shift increases reaching the maximal value $R^2_{sol} = 0.665$ at $\Omega \sim 0.11$ rad/s and then decreases, when vortex lines start to nucleate. This is the result of the interaction of the soliton with the counterflow $\vec{v}_s - \vec{v}_n$, where $\vec{v}_s$ and $\vec{v}_n = \vec{\Omega} \times \vec{r}$ are the superfluid and normal velocities correspondingly.

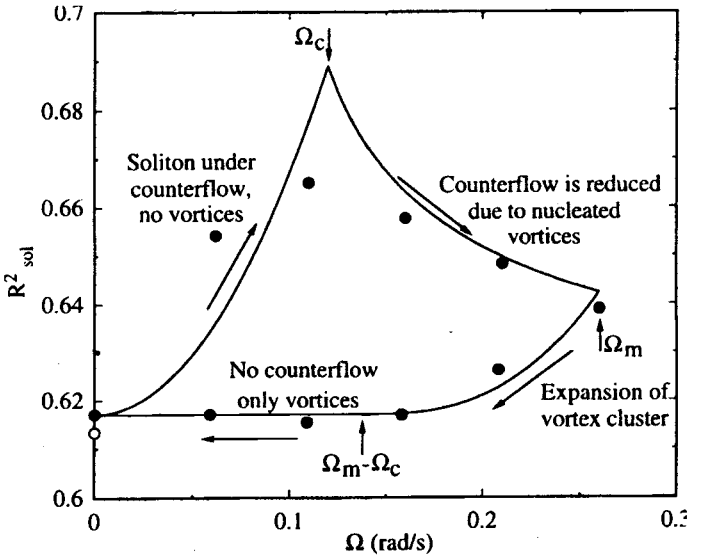

Fig.3. (•) The normalized frequency shift R^2_{sol} of the twist soliton satellite peak vs rotation velocity Ω, when the container is first accelerated from the stationary state to the maximum velocity $\Omega_m = 0.26$ rad/s and then decelerated to $\Omega = 0$. The initial value of R^2_{sol} is marked by (o). The hysteresis in R^2_{sol} reflects the influence of the counterflow $\vec{v}_s - \vec{\Omega} \times \vec{r}$ on the structure of the soliton. At the initial vortex-free stage, when $\vec{v}_s = 0$, the counterflow increases with Ω, which leads to the initial increase of R^2_{sol}. After the critical velocty Ω_c is reached, the conterflow region decreases when a cluster of vortices is formed. As a result R^2_{sol} decreases between Ω_c and Ω_m. During deceleration the conterflow region shrinks further until it disappers at $\Omega = \Omega_m - \Omega_c$. At still lower Ω, ie. in the absence of the counterflow, R^2_{sol} is nearly the same as in the stationary state.

The solid line is a theoretical fit assuming that the frequency shift of the soliton peak due to the counterflow is $\propto < (\vec{v}_s - \vec{v}_n)^2 >$, averaged over the soliton. In this fit we used for the nucleation threshold the value $\Omega_c = 0.12$ rad/s. The value $\Omega_c \sim 0.13$ rad/s was determined independently from the behavior of the vortex satellite

In the acceleration-deceleration cycle of Ω in Fig.3 four different phases are observed: (1) At first, when Ω is below the critical velocity $\Omega_c \sim 0.13$ rad/s of vortex nucleation, there are no vortices, and $\vec{v}_s = 0$. The counterflow $\vec{v}_s - \vec{v}_n = -\vec{\Omega} \times \vec{r}$ orients $\hat{l}$ parallel or antiparallel to the counterflow far from the soliton. Thus the total change of $\hat{l}$ across the soliton becomes 180^o. The orientational interaction of the counterflow with $\hat{l}$ leads to continuously shrinking width of the soliton wall

and the dimension of the attractive potential for the spin-waves decreases. As a result the spin-wave bound state is shifted closer to the continuum and $R^2_{\rm sol}$ increases with Ω.

(2) In the second phase, when $\Omega > \Omega_c$, vortices start to nucleate. These are the nonsingular 4π vortices with a dipole-unlocked core[17] which give rise to a satellite peak at $R^2_{\rm vortex} = 0.22 \pm 0.01$ (see Fig.2). Simultaneously $R^2_{\rm sol}$ starts to decrease because the vorticity reduces the width of the counterflow region. This shows that when $\Omega > \Omega_c$ a cluster of vortices is formed, where the vortices intersect the soliton (Fig.1).

(3) After reaching some arbitrary maximal velocity ($\Omega_m = 0.26$ rad/s in Fig.3) we start to decelerate the cryostat. Now the number of vortices is conserved, while the cluster expands and the counterflow decreases both in width and in magnitude. As a result $R^2_{\rm sol}$ decreases further until the counterflow finally disappears and the cluster reaches the wall of the container. Here the initial frequency shift of the soliton peak is restored.

(4) During further deceleration the counterflow region is absent and $R^2_{\rm sol}$ is nearly constant, which means that vortices cross an otherwise undisturbed composite twist soliton.

All four stages of this hysteretic behavior of $R^2_{\rm sol}(\Omega)$ can be reproduced theoretically (solid line in Fig.3) if one assumes that at low counterflow velocity the dependence $R^2_{\rm sol}(\Omega)$ is analytical: $R^2_{\rm sol}(\Omega) = R^2_{\rm sol}(0) + {\rm const} < (\vec{v}_s - \vec{v}_n)^2 >$, where the average is over the rotating container. From this experiment we conclude that an intersection with continuous (nonsingular) structure exists between a vortex line and a twist soliton. It can be formed reproducibly and exists for indefinite time as a metastable object in the rotating container.

Next we discuss the topology of the intersection of the twist soliton with the 4π vortex line along z. In the continuous 4π vortex the vorticity is produced by the nonsingular $\hat{\rm l}$ texture, which can be represented by a bound pair of Mermin-Ho (MH) 2π vortices, one with circular and the other with hyperbolic projection of $\hat{\rm l}$ in the xy plane (see [18], Review [17] and Fig.4). The $\hat{\rm l}$ texture within the vortex produces the $S^2 \to S^2$ mapping with index 1: the distribution of $\hat{\rm l}$ over the cross section of circular and hyperbolic MH vortices in the xy plane covers the north and south hemispheres of S^2 sphere $\hat{\rm l} \cdot \hat{\rm l} = 1$ respectively. The corresponding index of the $\hat{\rm d}$ texture is 0, because $\hat{\rm d}$ is kept in the xy plane by an axial magnetic field, thus in the vortex core $\hat{\rm l}$ and $\hat{\rm d}$ are unlocked. (In a lattice of 4π vortices one has periodic boundary conditions for $\hat{\rm l}$. Thus the $\hat{\rm l}$ texture within an elementary cell of the vortex lattice produces a mapping of the $2D$ torus $T^2 \to S^2$ with index 1. The whole A-phase order parameter is not periodic, it is invariant under "magnetic" translations: translations which are accompanied by the gauge transformation. As a result the counterflow $\vec{v}_s - \vec{\Omega} \times \vec{r}$ is periodic within the vortex lattice.)

What happens when such a vortex crosses the soliton? Far from the vortex, ie. within a pure soliton, $\hat{\rm l}$ is oriented in the transverse plane and its orientation depends on the vertical coordinate z: This serves as an asymptote for the intersection point, $\hat{\rm l}_{\rm asymptote}(z) = \hat{x}\cos\alpha(z) + \hat{y}\sin\alpha(z)$. If the vortices form a lattice, then α must change exactly by π when crossing the twist soliton, because far from the soliton the vortex lattice fixes $\hat{\rm l}$ parallel or antiparallel with respect to the lattice anisotropy axis[17]. The examples of topologically different intersections with given asymptotes far from the intersection can be embedded in the following

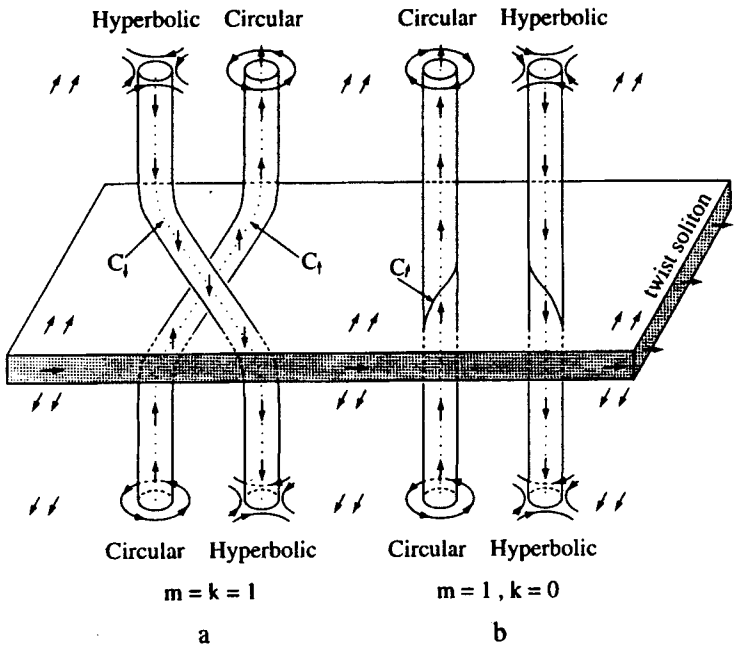

Fig.4. Two ways for the vortex to cross the soliton. (a) Intersection with topological indices $m = 1$, $k = 1$. $C_\uparrow$ and $C_\downarrow$ are loci of points where $\hat{\mathbf{l}}$ is up and down correspondingly. With two parallel twist solitons this texture is duplicated, and the two loops form a link. (b) Intersection with indices $m = 1$, $k = 0$. The same linking occurs between the loop $C_\uparrow$, for which $\hat{\mathbf{l}} = \hat{\mathbf{z}}$, and a neighbouring loop of constant $\hat{\mathbf{l}} \neq \hat{\mathbf{z}}$.

general serial with two integer parameters m and k, which will be later related to the topological invariants:

$$\hat{\mathbf{l}}_{m,k}(z, \vec{r}) = \mathrm{U}^m(z)\hat{\mathbf{l}}(-\infty, \mathrm{U}^k(z)\vec{r}) \quad . \tag{1}$$

Here $\vec{r}$ is the in-plane coordinate, counted, say, from the "center of mass" of the vortex pair; $\hat{\mathbf{l}}(-\infty, \vec{r})$ is the texture within the 4π vortex far from the soliton; and $\mathrm{U}(z)$ is the z-dependent matrix, which rotates $\hat{\mathbf{l}}$ within the twist soliton:

$$\mathrm{U}(z) = \begin{pmatrix} \cos\alpha(z) & \sin\alpha(z) & 0 \\ -\sin\alpha(z) & \cos\alpha(z) & 0 \\ 0 & 0 & 1 \end{pmatrix} \quad . \tag{2}$$

Index m shows an algebraic sum of the solitons, while k marks two competing intersections shown in Figs. 4(a) and 4(b), they have correspondingly $m = 1$, $k = 1$ and $m = 1$, $k = 0$. In the $m = 1$, $k = 1$ configuration the circular and hyperbolic MH vortices interchange after crossing the soliton making an entanglement, but do not change their orientation with respect to $\hat{\mathbf{l}}_{\mathrm{asymptote}}$. Vice versa, in the $m = 1$, $k = 0$ configuration the MH vortices do not interchange, but each MH vortex is twisted separately, and as a result the orientation of the whole 4π vortex with respect to $\hat{\mathbf{l}}_{\mathrm{asymptote}}$ changes to the opposite configuration. The latter means that the parity of the 4π vortex changes after crossing: the w^+ vortex transforms to its mirror reflected w^- modification in notations of [17].

This topological difference between the two textures can be described in terms of the linking numbers which usually characterize the π_3 homotopy [19], these linking numbers are related to the indices m and k. To visualize this let us consider two parallel identical solitons, this corresponds to $m = 2$ and even k in Eq.(1). After crossing two solitons the 4π vortex returns to its initial $\hat{\mathbf{l}}(-\infty, \vec{r})$ texture. This means that the cylinder $V_2 = T^2 \times (-\infty < z < +\infty)$, which crosses two solitons, represents the 3D torus, $V_2 = T^3$. Thus the $\hat{\mathbf{l}}$ texture within the cylinder produces the mapping $T^3 \to S^2$. This torus homotopy has no natural group structure[20], but nevertheless can be characterized by some integers.

Let us consider a loop C formed by the loci in space where the field $\hat{\mathbf{l}}$ takes a constant value. Let us take two values of $\hat{\mathbf{l}}$: one of them, $\hat{\mathbf{l}}_\uparrow$, is on the northern hemisphere and another one, $\hat{\mathbf{l}}_\downarrow$, is on the southern hemisphere. For example $\hat{\mathbf{l}}_\uparrow = \hat{z}$ and $\hat{\mathbf{l}}_\downarrow = -\hat{z}$. The corresponding loops are $C_\uparrow$ and $C_\downarrow$. Let us introduce the linking number $lk(C_\uparrow, C_\downarrow)$, which counts how often $C_\uparrow$ passes through $C_\downarrow$. One finds that it depends only on k, ie. $lk(C_\uparrow, C_\downarrow) = 1$ for the duplicated intersection with indices $m = 1$, $k = 1$ in Fig.4(a) and $lk(C_\uparrow, C_\downarrow) = 0$ for the duplicated intersection with indices $m = 1$, $k = 0$ in Fig.4(b).

Now let us consider two loops formed by loci, where $\hat{\mathbf{l}}$ takes two values on the same hemisphere (note that the $\hat{\mathbf{l}}$ texture in the circular and hyperbolic MH vortices covers the north and south hemispheres, respectively). Then the linking number of two loops of type $C_\uparrow$ is $lk(C_\uparrow, C_\uparrow) = -lk(C_\downarrow, C_\downarrow) = 1$ for the duplicated $m = 1$, $k = 0$ texture.

Let us express these integers in terms of analytical topological invariants. The Hopf index H, which is expressed in terms of the superfluid velocity [7]

$$H = \frac{1}{4\kappa^2} \int_{T^3} d^3r \ \vec{v}_s \cdot \vec{\nabla} \times \vec{v}_s \quad , \tag{3}$$

is not quantized in a given (open) geometry (here $\vec{v}_s = (\kappa/2\pi)\hat{\mathbf{e}}_1 \vec{\nabla} \hat{\mathbf{e}}_2$, $\Psi = \hat{\mathbf{e}}_1 + i\hat{\mathbf{e}}_2$ is the complex vector order parameter with $\hat{\mathbf{e}}_1 \times \hat{\mathbf{e}}_2 = \hat{\mathbf{l}}$; $\kappa = \pi\hbar/m_3$ is the circulation quantum in superfluid ^{3}He). This is because periodic boundary conditions are applied only to $\hat{\mathbf{l}}$ and $\vec{v}_s - \vec{v}_n$, but not to the whole order parameter: $\Psi(x, y, +\infty)$ is not necessarily equal to $\Psi(x, y, -\infty)$, this corresponds to a nonzero phase difference across the soliton, which is typical for Josephson contacts. The calculation of H for two identical solitons, ie for textures with double values of m and k, gives

$$H = \frac{1}{2}k + \frac{1}{2\kappa} \int_{C^*} d\vec{r} \cdot \vec{v}_s \quad , \tag{4}$$

where the last term corresponds to the phase difference and is expressed in terms of the circulation of $\vec{v}_s$ along the vertical path C^* on the lateral boundary of the cylinder. Eq.(4) means that the intersections in Fig.4(a) with nonzero $k = 1$ realizes the nontrivial π_3 topology.

For the intersections in Fig.4(b) the index $k = 0$, but the nontrivial topology of linking manifests itself in another analytical invariant, related to m. For the duplicated texture the circulation of $\vec{v}_s$ along the loop $C_\uparrow$ is different by one quantum from the calibrating circulation along C^*:

$$\left(\int_{C_\uparrow} - \int_{C^*}\right) d\vec{r} \cdot \vec{v}_s = +\kappa \quad . \tag{5}$$

Correspondingly $(\int_{C_\perp} - \int_{C^+})d\vec{r}\cdot\vec{v}_s = -\kappa$.

Which of the two types of intersection occurs depends on details of the hydrodynamic energy and therefore on temperature. A contribution to the energy difference between them comes also from the spontaneous axial supercurrent along the vortex core caused by broken parity of the w-vortex[17]. In the texture with $m = k = 1$ the vortex is in a single, say, w^+ state, therefore the axial current does not change direction on crossing the soliton. On the other hand, in the texture with $m = 1$, $k = 0$ the axial current is opposite for w^+ and w^- vortices on different sides of the solitons. The conservation law for the current requires that the intersection point is a source or sink for the mass current which flows from the vortices via the intersection point into the bulk liquid. The flow energy can make the $m = k = 1$ texture more advantageous. At the moment we cannot resolve between the two textures theoretically or experimentally.

In conclusion, the intersection of two continuous objects of different dimensionality, nonsingular $1D$ vortex and topological $2D$ soliton, is experimentally concluded to exist. Two competing types of intersection are described, which have different indices of π_3 homotopy.

This work was supported through the ROTA co-operation plan of the Finnish Academy and the Russian Academy of Sciences. G.E.V. was supported in part by the Russian Foundation for Fundamental Sciences, Grants No. 93-02-02687 and 94-02-03121; Ü.P. and V.M.H.R. enjoyed scholarships of the Finnish Cultural Foundation. G.E.V. thanks Yu. Makhlin and T. Misirpashaev for numerous discussions.

---

1. M.Kléman, Rep. Prog. Phys. **52**, *555* (1989); I.Chuang, N.Turok, and B.Yurke, Phys. Rev. Lett., **66**, 2472 (1991).
2. A.Vilenkin, Phys. Rep., **2**, 263 (1985); A.Vilenkin, and E.P.S.Shellard, *Cosmic Strings and Other Topological Defects* (Cambridge University Press, Cambridge,1993)
3. A.Malozemoff, and J.C.Slonczewski, *Magnetc Domain Walls in Bubble Materials* (New York: Academic 1979); Chih-Wen Chen, *Magnetism and Metallurgy of Soft Magnetic Materials* (North-Holland, Amsterdam 1977).
4. Y.Kondo, J.Korhonen, M.Krusius, V.Dmitriev, E.Thuneberg, and G.Volovik, Phys. Rev. Lett., **68**, 3331 (1992); Phys. Rev., **B 47**, 8868 (1993).
5. Ü.Parts, E.V.Thuneberg, G.E.Volovik, J.H.Koivuniemi, V.M.H.Ruutu, M.Heinilä, J.M.Karimäki, and M.Krusius, Phys. Rev. Lett., **72**, 3839 (1994).
6. Ü.Parts, J.H.Koivuniemi, M.Krusius, V.M.H.Ruutu , E.V.Thuneberg and G.E.Volovik, Pis'ma ZhETF, **59**, 816 (1994) [JETP Lett., **59**, 851 (1994)].
7. G.E.Volovik and V.P.Mineev, ZhETF **73**, 767 (1977) [Sov. Phys.: JETP, **46** 401 (1977)].
8. R.Shankar, J. Phys. (Paris), **38**, 1405 (1977).
9. T.-L.Ho, Phys. Rev., **B 18**, 1144 (1978).
10. J.A.Bryan, S.M.Caroll, and T.Pyne, Phys. Rev., **D 50**, 2806 (1994).
11. I.Chuang, R.Durrer, N.Turok, and B.Yurke, Science, **251**, 1336 (1991).
12. Y.Bouligand, J. Phys. (Paris), **35**, 959 (1974); Y.Bouligand, B.Derrida, V.Poenaru, Y.Pomeau, and G.Toulouse, J. Phys. (Paris), **39**, 863 (1978).
13. R.Kutka and H.R.Trebin, J. Physique Lett. (Paris), **45**, 1119 (1984).
14. A.M.Kosevich, B.A.Ivanov, and A.S.Kovalev, Phys. Rep., **194**, 117 (1990).
15. R.D.Pisarski, and D.L.Stein, J. Phys. (Paris), **41**, 345 (1980).
16. K.Maki and P.Kumar, Phys. Rev., **B 16**, 182 (1977).
17. For a review on vortices in ^{3}He see M.M.Salomaa, and G.E.Volovik, Rev. Mod. Phys., **59**, 533 (1987).
18. X.Zotos, and K.Maki, Phys. Rev., **B 30**, 145 (1984).
19. H.-R.Trebin, Adv. Phys., **31**, 195 (1982); L.Michel, Rev. Mod. Phys., **52**, 617 (1980).
20. A.T.Garel, J. Phys. (Paris), **39**, 225 (1978).